Cambrian edrioasteroid reveals new mechanism for secondary reduction of the skeleton in echinoderms

Samuel Zamora[1,2], Imran A. Rahman[3,4], Colin D. Sumrall[5], Adam P. Gibson[6] & Jeffrey R. Thompson[3,7]

[1]Instituto Geológico y Minero de España (IGME-CSIC), C/Manuel Lasala, 44, 9ºB, 50006, Zaragoza, Spain

[2]Grupo Aragosaurus-IUCA, Área de Paleontología, Facultad de Ciencias, Universidad de Zaragoza, Zaragoza, Spain

[3]Department of Earth Sciences, The Natural History Museum, Cromwell Road, London, SW7 5BD, United Kingdom

[4]Oxford University Museum of Natural History, Parks Road, Oxford, OX1 3PW, United Kingdom

[5]Department of Earth and Planetary Sciences, University of Tennessee, Knoxville, TN 37996-1526, USA

[6] Department of Medical Physics and Biomedical Engineering and Institute for Sustainable Heritage, University College London, Gower Street, London, WC1E 6BT, United Kingdom

[7]UCL Centre for Life's Origins and Evolution, University College London, Gower Street, London, WC1E 6BT, United Kingdom

Abstract

Echinoderms are characterized by a distinctive high-magnesium calcite endoskeleton as adults, but elements of this have been drastically reduced in some groups. Herein, we describe a new pentaradial echinoderm, *Yorkicystis haefneri* n. gen. n. sp., which provides the oldest evidence of secondary non-mineralization of the echinoderm skeleton. This material was collected from the Cambrian Kinzers Formation in York (Pennsylvania, USA) and is dated as *c*. 510 Ma. Detailed morphological observations demonstrate that the ambulacra (i.e. axial region) are composed of flooring and cover plates, but the rest of the body (i.e. extraxial region) is preserved as a dark film and lacks any evidence of skeletal plating. Moreover, X-ray fluorescence analysis reveals that the axial region is elevated in iron. Based on our morphological and chemical data and on taphonomic comparisons with other fossils from the Kinzers Formation, we infer that the axial region was originally calcified, while the extraxial region was non-mineralized. Phylogenetic analyses recover *Yorkicystis* as an edrioasteroid, indicating that this partial absence of skeleton resulted from a secondary reduction. We hypothesize that skeletal reduction resulted from lack of expression of the skeletogenic gene regulatory network in the extraxial body wall during development. Secondary reduction of the skeleton in *Yorkicystis* might have allowed for greater flexibility of the body wall.

Keywords: Cambrian, echinoderms, skeleton, evolution, development

1. Introduction

Animals are characterized by an enormous diversity of biomineralized skeletons, which perform important functions such as protecting the internal organs or supporting the body structure. Elucidating the origins of animal biomineralization is a major research focus in evolutionary and geobiology; skeletons are thought to have evolved independently in various clades during the latest Ediacaran or early Cambrian through co-option of a conserved ancestral genetic toolkit [1,2], with possible drivers including changing seawater chemistry, oxygen availability or increasing predation pressure [3,4]. However, the pattern and process of skeletal loss, widespread across animal phylogeny [5], is much less well studied, and it remains unclear if commonalities exist in how and why skeletons are reduced among species.

Echinoderms, with their distinctive high-magnesium calcite endoskeleton, are a model system for studying the evolution and development of the skeleton [6]. Calcareous plates or ossicles are ubiquitous in most echinoderm bodies, but the mineralized skeleton has been greatly reduced in some groups. For example, in derived crinoids the ambulacral flooring plates are decalcified [7], whereas in crown-group holothurians mineralization of the body-wall skeleton is mostly reduced to small spicules [8]. Thus, reduction of mineralization primarily affects distinct parts of the body in different classes; in crinoids, the axial region (i.e. parts of the body associated with the water vascular system) is most strongly affected, whereas in holothurians there is greater loss of mineralization in the extraxial region (i.e. the rest of the body). Although developmental mechanisms associated with skeletal formation are well understood in many echinoderms [9,10], the processes involved in skeletal reduction remain enigmatic. The reasons why some echinoderm groups reduced mineralization in their skeleton are also unclear, with explanations ranging from adaptation to more mobile lifestyles [11] to reducing the energetic cost of skeletogenesis [12].

Here, we describe a new echinoderm from the Cambrian of the USA, which has a unique body plan consisting of a calcified axial skeleton and a non-mineralized extraxial region. This taxon demonstrates that skeletal non-mineralization in echinoderms first occurred during the Cambrian, in a fundamentally different way to all other species.

2. Material and methods

Two specimens (NHMUK EE 1659, 1660), preserved as external moulds in laminated brown shale, were collected from the Emigsville Member of the Kinzers Formation in York, Pennsylvania, USA (for more information about this formation and fossil content, see [13]). Specimens were obtained from the south slope of the City View Church yard by Mr. Christopher Haefner in November 2018 (with permission from the church community). The coordinates of the exposure are 39.9842302 N, 76.7644671 W. At this locality, the Kinzers Formation crops out in a small tectonic block that includes the Emigsville and York members. Excavation yielded a rich associated fauna of trilobites, echinoderms (*Lepidocystis* and *Camptostroma*) and soft-bodied organisms (e.g. radiodontans). Echinoderms from this formation always show three-dimensional preservation of the skeleton. The Kinzers Formation extends from the middle Dyeran Stage to somewhere within the Delamaran Stage of the Laurentian zonation scheme for the Cambrian. The olenelloid trilobites *Wanneria walcottana* and *Olenellus roddyi* recovered from the City View Church site are consistent with this age assignment (Webster pers. comm. March 26, 2019). This falls within Stage 4 of the Cambrian in the global chronostratigraphic scale, approximately 510 Ma [14,15].

Specimens were photographed under natural light, both dry and submerged in water. To investigate the elemental distribution of the fossils, NHMUK EE 1659 was

analysed using a Bruker Tornado M4+ micro X-ray fluorescence (XRF) scanning spectrometer at University College London. Analysis with the Tornado M4+ was performed under a 2 mbar vacuum. The system has an X-ray tube with a rhodium target which was used with a 35 kV accelerating voltage and an 800 µA current. The dwell time was 100 µs, the resolution was 1228 × 888 pixels and the pixel size was 25 µm. The resulting fluorescence signal was detected using two silicon drift detector spectrometers. Lastly, specimens were cast in latex, with the resulting casts whitened with NH_4Cl sublimate prior to photography. Specimens are housed at the Natural History Museum of London, UK (NHMUK). Comparative material of other echinoderms from the Kinzers Formation is deposited in the Museum of Comparative Zoology (Harvard University) and National Museum of Natural History (Smithsonian Institution).

To establish the relationships between *Yorkicystis* and other early echinoderms, parsimony and Bayesian phylogenetic analyses were performed. We chose to focus exclusively on pentaradial forms because all recent phylogenetic analyses [16,17,18,19,20,21] have recovered these as derived in echinoderm phylogeny. We selected all the major pentaradial morphotypes present in the Cambrian and early Ordovician for which fossil material is sufficiently well known, including a spiral form (*Helicocystis*), early edrioasteroids (*Kailidiscus* and *Stromatocystites*), isorophid edrioasteroids (*Isorophus* and *Argodiscus*), plesiomorphic blastozoans (*Lepidocystis*, *Gogia*, and *Vyscystis*), an early glyptocystitid (*Ridersia*) and the earliest crinoids (*Titanocrinus* and *Apektocrinus*). *Helicoplacus* was chosen as the outgroup because it is a triradial form that is widely regarded as the sister group to pentaradial forms [17,22]. Morphological information was obtained from direct observations of fossil specimens and the published literature. Most of the taxa were coded as in previous phylogenetic

analyses [23,24,25]. The final character matrix consisted of 13 taxa and 28 characters (supplementary table 1). Parsimony analyses were run using the branch and bound algorithm in the program Paup* v. 4.0a [26]. Bayesian analyses were run using MrBayes v. 3.2 [27] using the Mkv model [28]. Rate variation was modeled using a gamma distribution with a prior of exponential (1.0). Branch lengths were unconstrained with a compound Dirichlet prior. Two differing values of the symmetric Dirichlet hyperprior were used to account for differing transition rate asymmetries. The joint posterior distribution of model parameters, branch lengths, and tree topologies was estimated using Markov chain Monte Carlo (MCMC). Additional details of phylogenetic analyses and MCMC convergence are provided in the supplementary information.

3. Results

(a) *Morphology of* Yorkicystis *gen. nov.*

The body of *Yorkicystis haefneri* gen. et sp. nov. is divided into two main regions that are preserved in different ways and correspond to the extraxial and axial body walls (*sensu* [29, 30]). The extraxial region of *Y. haefneri* gen. et sp. nov. consists of a globular body (figures 1*a*,*b*, 2*a*,*b*; supplementary material, figure S3), measuring 23 mm wide and 18 mm long in the most complete specimen (NHMUK EE 1659). It is preserved as a dark film (figure 2*a*), with no evidence of skeletal plating (figure 1*a*,*b*; supplementary material, figure S3). No attachment structure or body openings (e.g. periproct, gonopore, hydropore) are preserved.

The axial region is composed of five large, probably straight, recumbent ambulacra that converge in the peristomial region and presumably originate at the centrally located mouth (figures 1*a*,*b*, 2*a*,*b*). The ambulacra are long (maximum length

of 20 mm in the holotype and 24 mm in the paratype), wide in plan view, and slightly taper in width distally (figure 1*a–e*). Each ambulacrum is composed of two series of plates, which we interpret as flooring and cover plates, similar to those in other edrioasteroid-grade echinoderms [31]. Flooring plates are biserially arranged, triangular in shape, and very thick (figure 1*f–i*). Their internal surfaces are smooth, with notches at the lateral margins that we interpret as podial pores (*sensu* [32]) (figure 1*f,i*). Externally, these plates have prominent rims converging at a central point that extend to the corners of each plate (figure 1*c,d,e,g*). These rims are elevated compared to the main body of the plates. Cover plates are tessellate and organized into multiple series of tiny polygonal plates, which decrease in size towards the perradial line (figure 1*c–e*). The first series of cover plates articulate with the apices of the flooring plates. Ambulacra are preserved in reddish-orange (figure 2*a*). The peristome is covered by tiny plates with no obvious organization preserved (figure 1*a,b*).

(b) ***Elemental analysis***

XRF mapping showed that NHMUK EE 1659 is enriched in P, Fe, Ca, Zn and S and depleted in Si, Al, K and Mg compared to the surrounding matrix (figure 2*b*; supplementary material, figure S2). Within the fossil, the axial region is especially elevated in Fe (figure 2*b*; supplementary material, figure S2), with local enrichment of Zn and S in some parts (supplementary material, figure S2); P and Ca are elevated in both the axial and extraxial regions (figure 2*b*; supplementary material, figure S2).

(c) ***Phylogenetic position***

In both our Bayesian and parsimony analyses, *Yorkicystis* was recovered as an edrioasteroid, in a clade with *Argodiscus*, *Isorophus*, and *Kailidiscus* (figure 3). This

clade of edrioasteroids was part of a larger clade consisting of all pentaradial forms excluding *Helicocystis*. In both analyses, *Helicocystis* was retrieved as the earliest-diverging pentaradial echinoderm.

4. Discussion

Variation in the morphology and preservation of the axial and extraxial parts of the body in *Yorkicystis* demonstrates that these regions had different compositions in life. While the specimens preserve no trace of original calcite, the presence of ambulacra with characteristic flooring and cover plates (figures 1*c–i*, 4), preserved as 3-dimensional moulds elevated in Fe (figure 2*b*; supplementary material, figure S2), and the relict 'ghost' stereom microstructure in the external part of flooring plates are clear indicators of a typical echinoderm skeleton. In contrast, the extraxial region is generally preserved as a dark film (figure 2*a*). This mode of preservation is common among Burgess Shale-type deposits like the Kinzers Formation [33, 34], and soft tissues are often preserved in this way [33, 35]. This, together with the apparent absence of skeletal plating, as revealed by direct study of the fossils and latex casting (figures 1*a*,*b*, 2*a*,*b*; supplementary material, figure S3), strongly suggests the extraxial region of *Yorkicystis* was originally non-mineralized. Although the fossils appear preserved flattened and with curved ambulacra, taphonomic observations indicate that their original shape was globular and probably with straight ambulacra (supplementary material, figure S1).

Our phylogenetic analyses recover *Yorkicystis* as an edrioasteroid (figure 3), revealing that the reduction of the skeleton was a derived trait, and not representative of the plesiomorphic condition among pentaradial echinoderms. *Yorkicystis* is thus interpreted as the oldest echinoderm with a secondarily non-mineralized body wall (figure 5). While a small number of Ediacaran and lower Cambrian fossils have

196 previously been considered as uncalcified echinoderms (e.g. [18,36,37,38]), their
197 echinoderm affinities are highly dubious and debated [20,22,39,40]. However,
198 comparable patterns of incomplete calcification have been documented in other
199 echinoderm groups based on younger fossil and living forms. For example, in most
200 crinoids, flooring plates are weakly or not calcified, while other elements of the axial
201 skeleton are mineralized [7, 41]; in some taxa, components of the extraxial region, such
202 as the anal sac, are also uncalcified [12]. Some edrioasteroids like isorophids and
203 *Walcottidiscus* also reduce part of the aboral region to attach on substrates [42]. More
204 radical reduction of skeletal mineralization is present among holothurians, in which the
205 skeleton typically consists of small spicules embedded in the body wall and a ring of
206 ossicles surrounding the pharynx [8,43], or is lost entirely [11, 44]; skeletal reduction
207 thus affects both the axial and extraxial regions. Consequently, *Yorkicystis* is unique
208 among echinoderms in having a clear differentiation between calcified axial and
209 uncalcified extraxial regions.
210 Developmental mechanisms underpinning the formation of the skeleton in
211 *Yorkicystis* may shed light on skeletal development in echinoderms more broadly.
212 Transcriptomic comparisons of crinoids, echinoids, asteroids, and ophiuroids [10], as
213 well as numerous experimental studies in larval and adult skeletons of extant
214 echinoderm classes, have identified a conserved biomineralization ‘toolkit’ of genes and
215 proteins that underlies the process of skeletogenesis. This includes transcription factors
216 such as Alx1 and Ets1, signalling pathways like FGF and VEGF, and numerous
217 downstream differentiation genes such as c-lectin protein domain-bearing genes,
218 metalloproteases, and cell-surface molecules [9,10,45,46]. The existence of this
219 conserved set of genes across echinoderms points to a distinct genetic regulatory
220 module directing the development of the echinoderm skeleton. During development,

aspects of this regulatory network are deployed in distinct spatial contexts based on ectodermal signalling cues, resulting in the growth of skeleton in particular parts of the body [45–48]. Inhibiting these signalling pathways results in downregulation of skeletogenic genes, and obstruction of biomineralization in both embryos and adult echinoderms [46–48]. Given the conserved nature of the main components of the echinoderm skeletal biomineralization toolkit, we expect that the echinoderm skeletal gene regulatory network has been expressed during skeletal growth in both axial and extraxial skeletons of all fossil echinoderms. We hypothesize that, where this skeletogenic module is not deployed, skeletal loss or reduction will result. In this context, *Yorkicystis*, with its uncalcified extraxial body, indicates that components of the skeletogenic gene regulatory network were expressed only in the axial region.

The morphology of *Yorkicystis* could also indicate that the activation of the skeletogenic gene regulatory network in axial and extraxial tissues is independent and that the expression of this gene network in these tissues may be controlled by different upstream developmental genetic mechanisms, such as differential deployment of signalling pathways. This might imply different molecular mechanisms underlying the development of axial and extraxial tissue [49], although the existence of other echinoderms with varying degrees of calcification across axial and extraxial regions (see above) could point to greater variability in developmental processes between taxa. Recent advances in CRISPR genome editing have facilitated functional perturbations of gene expression in adult echinoderms in distinct morphological regions of the adult body plan [50]. Based on the morphology of *Yorkicystis*, with its calcified axial and uncalcified extraxial skeletons, we hypothesize that that functional knockout of transcription factors or signalling genes toward the top of the skeletal gene regulatory network hierarchy, such as *Alx1* or *VegfR*, in the extraxial regions of growing adult

246 echinoderms will result in a distinct loss of skeleton in those regions. Developments in
247 functional perturbations, paired with recent advances in localizing skeletal gene
248 expression in post-metamorphic echinoderms [51], make testing this hypothesis
249 possible.

250 Early echinoderms displayed great plasticity in terms of their body-plan
251 construction, with bilateral, asymmetrical, triradial and pentaradial forms described
252 from the Cambrian [22,52]. Recent phylogenetic analyses [18,20,17,19] place bilateral
253 and asymmetrical forms as stem-group echinoderms, indicating that some of the
254 synapomorphies of crown-group echinoderms, such as pentaradial symmetry and
255 ambulacra with flooring and cover plates, are not plesiomorphic for the phylum [16,22].
256 Our phylogenetic analyses recover *Yorkicystis* as a derived pentaradial form, most
257 closely related to Cambrian edrioasteroids such as *Kailidiscus*, with the absence of
258 skeleton in the extraxial part of the body due to secondary loss. This represents the
259 oldest example of skeletal reduction yet documented in echinoderms. Moreover, the
260 secondary loss of skeleton in the extraxial region alone differs from the situation in all
261 other echinoderms with reduced skeletons (e.g. crinoids and holothurians), and strongly
262 implies a distinct mechanism for reducing the skeleton. The absence of skeleton in the
263 extraxial region suggests that *Yorkicystis* preferentially directed energy towards
264 skeletogenesis in the axial region. This would have conserved energy for other
265 metabolic requirements, while still ensuring the external soft parts of the water vascular
266 system (i.e. the tube feet, figure 4*k*) were supported and protected. The absence of
267 plating in the extraxial part would also explain why the ambulacra in *Yorkicystis* depart
268 morphologically from other edrioasteroids. Loss of the extraxial skeleton might have
269 enabled greater flexibility of the body wall, allowing the animal to vary its body shape
270 in response to changing currents.

5. Systematic palaeontology

Phylum: Echinodermata

Class: Edrioasteroidea

Family: Yorkicystitidae nov.

Genus: *Yorkicystis* gen. nov.

Type species: *Yorkicystis haefneri* sp. nov.

Etymology. Genus name refers to the city of York, Pennsylvania, where specimens were collected.

Diagnosis. Extraxial body uncalcified. Axial body composed of five large, recumbent ambulacra incorporated into the thecal wall. Ambulacra consist of biserially arranged, large triangular adradial flooring plates with external rims; flooring plates internally smooth, with podial pores along lateral margins. Cover plates organized into multiple series.

Discussion. The new family Yorkicystitidae is here created to accommodate the new genus and species *Yorkicystis haefneri*, which is differentiated from all other edrioasteroids based on its unique body construction (uncalcified extraxial region and ambulacral construction). The ambulacra, consisting of multiple series of cover plates and biserial flooring plates, differ from those of derived isorophid edrioasteroids, which have uniserial flooring plates [23,53], but are more similar to stromatocystitids (i.e. *Cambraster* and *Stromatocystites*) and edrioasterids in which flooring plates are biserially arranged [32,42,54,55]. The flooring plate system in

Yorkicystis probably corresponds to and is thus homologous with the adradial series of *Walcottidiscus* [42]. In *Cambraster*, *Stromatocystites*, and edrioasterids the flooring plates are externally exposed and articulate aborally with the tessellate interambulacral membrane; this is not the case in *Yorkicystis* because of the absence of calcified elements in the extraxial region. But the floor plates do not have an externally exposed shelf that would be expected if they were the abradial set. Instead they are strongly rimmed in *Yorkicystis*.

The cover plate system in *Yorkicystis* is similar to the multitiered systems in some other Cambrian echinoderms, including the edrioasteroid *Kailidiscus* and the class Cincta, where larger platelets abradially articulate with tiers of smaller platelets towards the midline. This type of cover plate system is unknown among taxa with biserial abradial floor plates, except for the edrioasterid *Pseudedriophus guensburgi*, which is otherwise dissimilar [56].

Yorkicystis haefneri sp. nov.

Etymology. Species name dedicated to Mr. Christopher Haefner, who discovered the two known specimens and made them available for research.

Diagnosis. As for genus.

Material. Holotype: NHMUK EE 1659, includes part and counterpart. Paratype: NHMUK EE 1660, is a complete specimen with well preserved ambulacra.

Locality and horizon. York, Pennsylvania, USA; Stage 4, Series 2, Cambrian.

Description. See above and supplementary information.

Data accessibility. Data from elemental analysis are available from the Dryad Digital Repository: XXXXXXXXX [REF].

Authors' contributions. S.Z. conceived the study, cast and photographed specimens, conceived the phylogenetic analysis, analysed and interpreted data, and drafted the manuscript. I.A.R. conceived the elemental analysis, helped draft the manuscript, analysed and interpreted data, and critically revised the manuscript. C.D.S. conceived the phylogenetic analysis, analysed and interpreted data and critically revised the manuscript. J.R.T. ran the phylogenetic analyses, analysed and interpreted data and critically revised the manuscript. A.P.G. conceived and carried out the elemental analysis, analysed and interpreted data, and critically revised the manuscript. All authors gave final approval for publication and agree to be held accountable for the work performed therein.

Competing interests. We declare we have no competing interests.

Funding. S.Z. was supported by the Spanish Ministry of Science, Innovation and Universities (CGL2017-87631), co-financed by the European Regional Development Fund and the project "Aragosaurus: Recursos Geológicos y Paleoambientales" (E18_17R) funded by the Government of Aragon. I.A.R. was supported by Oxford University Museum of Natural History. J.R.T. was supported by a Royal Society Newton International Fellowship and a Leverhulme Trust Early Career Fellowship.

Acknowledgements. We thank Julia Sigwart, Bill Ausich and three anonymous reviewers for critical comments that improved the manuscript. We are grateful to Mr. Christopher Haefner for collecting and making the fossil specimens available for research, the City View Church community for giving permission to collect material from their premises, and Vinay Patel, Duncan Murdock and Tobias Salge for assistance with elemental analyses and discussion of results. Isabel Pérez helped with photographs of the paper, Fernando A. Ferratges prepared one of the specimens, and Tim Ewin curated the material and provided specimen numbers. Hugo Salais (Metazoa Studio) created the images used in figures 3, 4 and S1. Finally, Prof. Roger D. K. Thomas is thanked for being very supportive of our work.

References

1. Ewin DH. 2020 The origin of animal body plans: a view from fossil evidence and the gene regulatory genome. *Development* **147**, dev182899. (doi:10.1242/dev.182899)
2. Murdock DJE. 2020 The “biomineralization toolkit” and the origin of animal skeletons. *Biol. Rev.* **95**, 1372–1392. (doi:10.1111/brv.12614)
3. Wood R, Ivantsov AY, Zhuravlev AY. 2017 First macrobiota biomineralization was environmentally triggered. *Proc. R. Soc. B* **284**, 20170059. (doi:10.1098/rspb.2017.0059)
4. Wood R. 2018 Exploring the drivers of early biomineralization. *Emerg. Top. Life Sci.* **2**, 201–212. (doi:10.1042/ETLS20170164)
5. Nielsen C. 2011 Animal Evolution: Interrelationships of the Living Phyla. Oxford University Press, 416 pp.

6. Cary GA, Hinman VF. 2017 Echinoderm development and evolution in the post-genomic era. *Dev. Biol.* **427**, 203–211. (doi:10.1016/j.ydbio.2017.02.003)
7. Guensburg TE, Sprinkle J. 2009 Solving the mystery of crinoid ancestry: new fossil evidence of arm origin and development. *J. Paleontol.* **83**, 350–364. (doi:10.1666/08-090.1)
8. Smith AB, Reich M. 2013 Tracing the evolution of the holothurian body plan through stem group fossils. *Biol. J. Linn. Soc.* **109**, 670–681. (doi:10.1111/bij.12073)
9. Gao F, Thompson JR, Petsios E, Erkenbrack E, Moats RA, Bottjer DJ, Davidson EH, 2015 Juvenile skeletogenesis in anciently diverged sea urchin clades. *Dev. Biol.* **400**, 148–158. (doi:10.1016/j.ydbio.2015.01.017)
10. Dylus DV, Czarkwiani A, Blowes LM, Elphick MR, Oliveri P. 2018 Developmental transcriptomics of the brittle star *Amphiura filiformis* reveals gene regulatory network rewiring in echinoderm larval skeleton evolution. *Genome Biol.* **19**, 26. (doi:10.1186/s13059-018-1402-8).
11. Smirnov AV. 2016. Parallelisms in the evolution of sea cucumbers (Echinodermata: Holothuroidea). *Paleontol. J.* **50**, 1610–1625.
12. Kammer TW, Ausich WI. 2007 Soft-tissue preservation of the hind gut in a new genus of cladid crinoid from the Mississippian (Visean, Asbian) at St Andrews, Scotland. *Palaeontology* **50**, 951–959. (doi:10.1111/j.1475-4983.2007.00687.x)
13. Thomas RDK, Runnegar B, Matt K. 2020 *Pelagiella exigua*, an early Cambrian stem gastropod with chaetae: lophotrochozoan heritage and conchiferan novelty. *Palaeontology* **63**, 601–627. (doi:10.1111/j.1475-4983.2007.00687.x)

14. Sundberg FA, Geyer G, Kruse PD, McCollum LB, Pegel TV, Żylińska A, Zhuravlev AY. 2016 International correlation of the Cambrian Series 2-3, Stages 4-5 boundary interval. *Australas*. *Palaeontol*. *Mem*. **49**, 83–124.
15. Geyer G. 2019 A comprehensive Cambrian correlation chart. *Episodes* **42**, 321–332. (doi:10.18814/epiiugs/2019/019026)
16. Zamora S, Rahman IA, Smith AB. 2012 Plated Cambrian Bilaterians Reveal the Earliest Stages of Echinoderm Evolution. *PLoS One* **7**, e38296. (doi:10.1371/journal.pone.0038296)
17. Smith AB, Zamora S. 2013 Cambrian spiral-plated echinoderms from Gondwana reveal the earliest pentaradial body plan. *Proc*. *R*. *Soc*. *B* **280** 20131197. (doi:10.1098/rspb.2013.1197)
18. Topper TP, Guo J, Clausen S, Skovsted CB, Zhang Z. 2019 A stem group echinoderm from the basal Cambrian of China and the origins of Ambulacraria. *Nat*. *Commun*. **10**, 1366. (doi:10.1038/s41467-019-09059-3)
19. Nanglu K, Caron JB, Cameron CB. 2020 Cambrian tentaculate worms and the origin of the hemichordate body plan. *Curr. Biol.* 30, 4238–4244.e1. (doi:10.1016/j.cub.2020.07.078)
20. Zamora S, Wright DF, Mooi R, Lefebvre B, Guensburg TE, Gorzelak P, David B, Sumrall CD, Cole SR, Hunter AW, Sprinkle J, Thompson JR, Ewin TAM, Fatka O, Nardin E, Reich M, Nohejlová M, Rahman IA. 2020 Re-evaluating the phylogenetic position of the enigmatic early Cambrian deuterostome *Yanjiahella*. *Nat*. *Commun*. **11**, 1286. (doi:10.1038/s41467-019-09059-3)
21. Hunter AW, Ortega-Hernández J. 2021 A new somasteroid from the Fezouata Lagerstätte in Morocco and the Early Ordovician origin of Asterozoa. *Biol*. *Lett*. **17**, 20200809. (doi:10.1098/rsbl.2020.0809)

22. Zamora S, Rahman IA. 2014 Deciphering the early evolution of echinoderms with Cambrian fossils. *Palaeontology* **57**, 1105–1119. (doi:10.1111/pala.12138)
23. Sumrall CD, Zamora S. 2011 Ordovician edrioasteroids from Morocco: Faunal exchanges across the Rheic Ocean. *J. Syst. Palaeontol.* **9**, 425–454. (doi:10.1080/14772019.2010.499137)
24. Zamora S, Smith AB. 2012 Cambrian stalked echinoderms show unexpected plasticity of arm construction. *Proc. R. Soc. B* **279**, 293–298. (doi:10.1098/rspb.2011.0777)
25. Nohejlová M, Nardin E, Fatka O, Kašička L, Szabad M. 2019 Morphology, palaeoecology and phylogenetic interpretation of the Cambrian echinoderm Vyscystis (Barrandian area, Czech Republic). *J. Syst. Palaeontol.* **17**, 1619–1634. (doi:10.1080/14772019.2018.1541485)
26. Swofford DL. 2002 PAUP*. *Phylogenetic analysis using parsimony (*and other methods). Version 4*. Sunderland, MA: Sinauer Associates.
27. Ronquist F, Teslenko M, van der Mark P, Ayres DL, Darling A, Höhna S, Larget B, Liu L, Suchard MA, Huelsenbeck, JP. 2012 MrBayes 3.2: efficient Bayesian phylogenetic inference and model choice across a large model space. *Syst. Biol.* **61**, 539–542. (doi:10.1093/sysbio/sys029)
28. Lewis PO. 2001 A likelihood approach to estimating phylogeny from discrete morphological character data. *Syst. Biol.* **50**, 913–925 (doi:10.1080/106351501753462876)
29. Mooi R, David B, Marchand D. 1994 Echinoderm skeletal homologies: classical morphology meets modern phylogenetics. In *Echinoderms through time* (eds B David, A Guille, JP Féral, M Roux), pp. 87–95. Rotterdam, The Netherlands: Balkema.

30. David B, Mooi R. 1998 Major events in the evolution of echinoderms viewed by the light of embryology. In *Echinoderms: San Francisco* (eds R Mooi, M. Telford), pp. 21–28. Rotterdam, The Netherlands: Balkema.
31. Bell BM. 1976 A study of North American Edrioasteroidea. *N. Y. State Mus. Mem.* **21**, 446 pp.
32. Smith AB. 1985 Cambrian eleutherozoan echinoderms and the early diversification of edrioasteroids. *Palaeontology* **28**, 715–756.
33. Gaines RR, Briggs DEG, Yuanlong Z. 2008 Cambrian Burgess Shale-type deposits share a common mode of fossilization. *Geology* **36**, 755–758. (doi:10.1130/G24961A.1)
34. Butterfield NJ. 1995 Secular distribution of Burgess-Shale-type preservation. *Lethaia* **28**, 1–13. (doi:10.1111/j.1502-3931.1995.tb01587.x)
35. Walcott CD. 1911 Middle Cambrian holothurians and medusa. *Smithson. Misc. Collect.* **57**, 41–68.
36. Gehling JG. 1987 Earliest known echinoderm — a new Ediacaran fossil from the Pound Subgroup of South Australia. *Alcheringa* **11**, 337–345.
37. Shu D-G, Conway Morris S, Han J, Zhang Z-F, Liu J-N. 2004 Ancestral echinoderms from the Chengjiang deposits of China. *Nature* **430**, 422–428. (doi:10.1038/nature02648)
38. Swalla BJ, Smith AB. 2008 Deciphering deuterostome phylogeny: molecular, morphological and palaeontological perspectives. *Phil. Trans. R. Soc. B* **363**, 1557–1568. (doi:10.1098/rstb.2007.2246)
39. Clausen S, Hou X-G, Bergström J, Franzén C. 2010 The absence of echinoderms from the Lower Cambrian Chengjiang fauna of China:

palaeoecological and palaeogeographical implications. *Palaeogeogr. Palaeoclimatol. Palaeoecol.* **294**, 133–141. (doi:10.1016/j.palaeo.2010.01.001)

40. Topper TP, Guo J, Clausen S, Skovsted CB, Zhang Z. 2020 Reply to 'Re-evaluating the phylogenetic position of the enigmatic early Cambrian deuterostome *Yanjiahella*'. *Nat. Commun.* **11**, 1287. (doi:10.1038/s41467-020-14922-9)
41. Guensburg TE, Sprinkle J, Mooi R, Lefebvre B, David B, Roux M, Derstler K. 2020 *Athenacrinus* n. gen. and other early echinoderm taxa inform crinoid origin and arm evolution. *J. Paleontol.* **94**, 311–333. (doi:10.1017/jpa.2019.87)
42. Zhao Y, Sumrall CD, Parsley RL, Peng J. 2010 *Kailidiscus*, a new plesiomorphic edrioasteroid from the basal Middle Cambrian Kaili Biota of Guizhou Province, China. *J. Paleontol.*, **84**, 668–680. (doi:10.1017/S0022336000058388)
43. Rahman IA, Thompson JR, Briggs DEG, Siveter DJ, Siveter DJ, Sutton MD. 2019 A new ophiocistioid with soft-tissue preservation from the Silurian Herefordshire Lagerstätte, and the evolution of the holothurian body plan. *Proc. R. Soc. B* **286**, 20182792. (doi:10.1098/rspb.2018.2792)
44. Martins L, Souto C. 2020 Taxonomy of the Brazilian Apodida (Holothuroidea), with the description of two new genera. *Marine Biology Research* **16**, 219–255. (doi: 10.1080/17451000.2020.1761027)
45. Gao F, Davidson EH. 2008 Transfer of a large gene regulatory apparatus to a new developmental address in echinoid evolution. *Proc. Natl. Acad. Sci. U.S.A.* **105**, 6091–6096. (doi:10.1073/pnas.0801201105)

46. Czarkwiani A, Dylus DV, Carballo L, Oliveri P. 2019 FGF signalling plays similar roles in development and regeneration of the skeleton in the brittle star *Amphiura filiformis*. *Development* **148**, dev180760. (doi:10.1242/dev.180760)
47. Duloquin L, Lhomond G, Gache C. 2007 Localized VEGF signaling from ectoderm to mesenchyme cells controls morphogenesis of the sea urchin embryo skeleton. *Development* **134**, 2293–2302. (doi:10.1242/dev.005108)
48. Morgulis M, Gildor T, Roopin M, Sher N, Malik A, Lalzar M, Dines M, de-Leon SBT, Khalaily L, de-Leon SBT. 2019 Possible cooption of a VEGF-driven tubulogenesis program for biomineralization in echinoderms. *Proc. Natl. Acad. Sci. U.S.A.* **116**, 12353–12362. (doi:10.1073/pnas.1902126116)
49. Mooi R, David B, Wray GA. 2005 Arrays in rays: terminal addition in echinoderms and its correlation with gene expression. *Evol. Dev.* **7**, 542–555. (doi:10.1111/j.1525-142X.2005.05058.x)
50. Wessel GM, Kiyomoto M, Shen T-L, Yajima, M. 2020 Genetic manipulation of the pigment pathway in a sea urchin reveals distinct lineage commitment prior to metamorphosis in the bilateral to radial body plan transition. *Sci. Rep.* **10**, 1973. (doi:10.1038/s41598-020-58584-5)
51. Thompson JR, Paganos P, Benvenuto G, Arnone MI, Oliveri P. 2021 Post-metamorphic skeletal growth in the sea urchin *Paracentrotus lividus* and implications for body plan evolution. *EvoDevo* **12**, 3. (doi:10.1186/s13227-021-00174-1)
52. Smith AB, Zamora S, Álvaro JJ. 2013. The oldest echinoderm faunas from Gondwana show that echinoderm body plan diversification was rapid. *Nat. Commun.* **4**, 1385. (doi:10.1038/ncomms2391)

53. Kammer TW, Sumrall CD, Ausich WI, Deline B, Zamora S. 2013 Oral region homologies in Paleozoic crinoids and other plesiomorphic pentaradial echinoderms. *PLoS One* **8**, e77989. (doi:10.1371/journal.pone.0077989)
54. Zamora S, Sumrall CD, Vizcaïno D. 2013 Morphology and ontogeny of the Cambrian edrioasteroid echinoderm *Cambraster cannati* from western Gondwana. *Acta Palaeontol. Pol.* **58**, 545–559. (doi:10.4202/app.2011.0152)
55. Zamora S, Lefebvre B, Hosgör I, Franzen C, Nardin E, Fatka O, Álvaro JJ. 2015 The Cambrian edrioasteroid *Stromatocystites* (Echinodermata): systematics, palaeogeography and palaeoecology. *Geobios* **48**, 417–426. (doi:10.1016/j.geobios.2015.07.004)
56. Sprinkle J, Sumrall CD. 2015 New edrioasterine and astrocystitid (Echinodermata: Edrioasteroidea) from the Ninemile Shale (Lower Ordovician), central Nevada. *J. Paleontol.* **89**, 346–352. (doi:10.1017/jpa.2014.29)

Figure captions

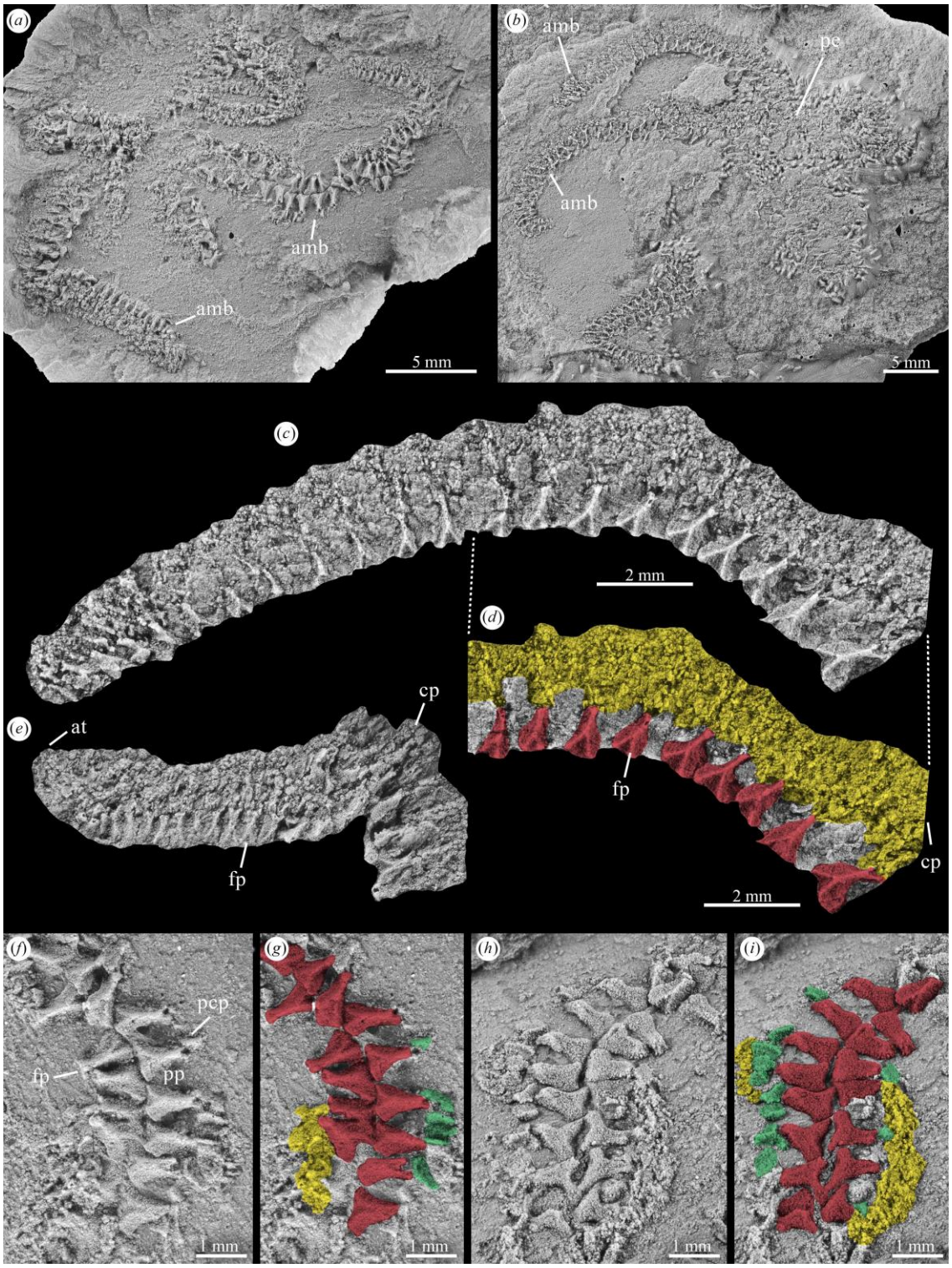

Figure 1. *Yorkicystis haefneri* from the early Cambrian Kinzers Formation (York, Pennsylvania). (*a*) NHMUK EE 1659, holotype complete specimen. (*b*) NHMUK EE 1660, paratype complete specimen. (*c*,*d*) NHMUK EE 1660, ambulacrum in lateral view. (*e*) NHMUK EE 1659, ambulacrum in lateral view. (*f*–*i*). NHMUK EE 1659, ambulacrum in plan view, part (*f*,*g*) and counterpart (*h*,*i*). Colours: red, flooring

plates; green, primary of cover plates; yellow, cover plates. Abbreviations: amb, ambulacrum; at, ambulacral tip; cp, cover plate; fp, flooring plate; pcp, primary cover plate; pe, peristome; pp, podial pore. All images are photographs of latex casts whitened with NH_4Cl sublimate.

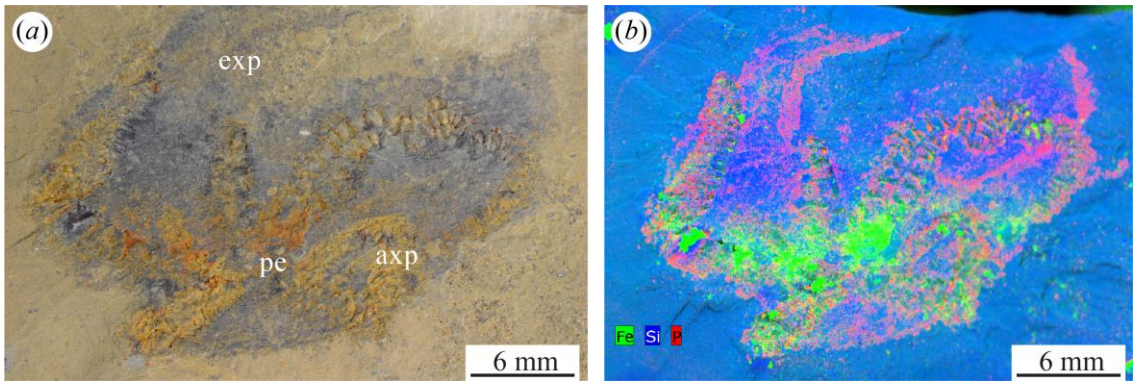

Figure 2. *Yorkicystis haefneri* from the early Cambrian Kinzers Formation (York, Pennsylvania). (NHMUK EE 1659). (*a*) Photograph of specimen submerged in water. (*b*) False-colour element map generated using X-ray fluorescence analysis showing Fe (green), Si (blue) and P (red); intensity of colour corresponds to element intensity. Abbreviations: axp, axial part; exp, extraxial part; pe, peristome.

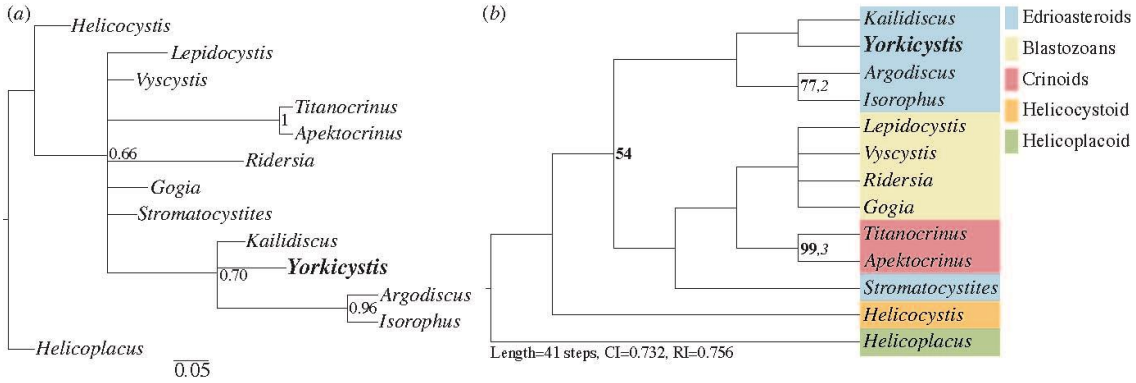

Figure 3. Phylogenetic position of *Yorkicystis*. (a) 50% majority-rule consensus tree resulting from Bayesian analyses. Numbers next to nodes represent the proportion of trees in the post-burn in posterior sample that contained that node. Analysis performed with a symmetric Dirichelet hyperprior set to ∞, corresponding to symmetric character transition rates. Branch lengths represent the number of expected changes per character. (b) Strict consensus of the four most parsimonious trees resulting from parsimony analyses. Bootstrap support (BS; bold) and decay indices (DI; italics) are shown for each node with BS > 50 and DI > 0.Both trees are rooted on *Helicoplacus*.

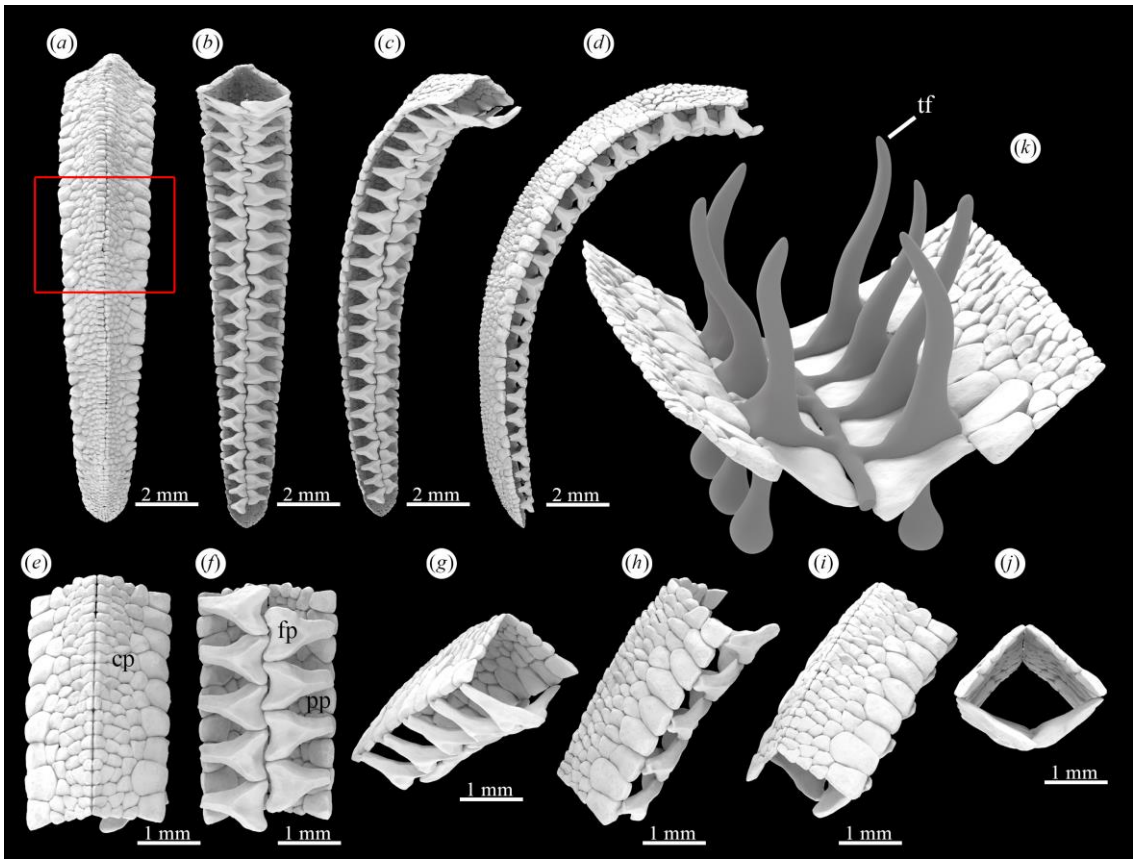

Figure 4. Digital reconstruction of the ambulacral construction of *Yorkicystis haefneri*. (*a*–*d*) Single ambulacrum in different views. (*e*–*j*) Detail of part of the ambulacrum in different views. (*k*) Inferred soft tissues of the water vascular system housed within the ambulacrum during life. Abbreviations: cp, cover plate; fp, flooring plate; pp, podial pore; tf, tube foot.

Figure 5. Life reconstruction of *Yorkicystis haefneri*.

Electronic supplementary material

Supplementary Information. The supplementary information of this paper includes taphonomic observations, additional results from X-ray fluorescence analysis, a full description of the fossils and further details on the phylogenetic analyses. Supplementary table 1 includes character states for all taxa included in the phylogenetic analyses.